

Rotational Components of Strong-motion Earthquakes

Vincent W Lee¹ and Jianwen Liang²

¹ Professor, Civil & Environmental Engineering, Univ. of Southern California, Los Angeles, CA 90089 USA, vlee@usc.edu

² Professor, School of Civil Engineering, Tianjin University, Tianjin 300072, China, liang@tju.edu.cn

ABSTRACT :

The rotational components associated with the dynamic response of elastic and of poro-elastic half space can be as important as the actual deformations, for computation of the response of the half space and for the response analyses of engineering structures, and must be included in all analyses.

The basic theory of elasticity shows that the Eulerian strain tensor of deformations is expressible in terms of the linear strain tensor and the second order terms of rotation tensor. At present, all structural analyses already deal with the generalized displacement of the 3 components of translations and the 3 components of rotations as the 6 independent components. These six generalized components are often simultaneously estimated using the kinematic equations of forces and moments. Since rotations are defined in terms of derivatives of translations, with respect to space coordinates, there always should exist analytic expressions for rotations in terms of the translations. This is certainly the case when the translation components are given in rectangular coordinates.

Using surface waves, the method of Trifunac (1971) for generating artificial, synthetic strong motion accelerograms can thus immediately be extended to generate both synthetic torsional and rocking accelerograms and of their response spectra (Lee and Trifunac, 1985, 1987, 2008). Those are constructed from the horizontal and vertical acceleration components. These rotational components of strong ground motions are gaining attention as it is becoming evident that they can contribute significantly to the overall response of structures during strong earthquake motions.

This paper intends to stress the importance of the rotational components of accelerograms, to develop theories and algorithms for generating rotational motions from the corresponding available translational motions, and to check such validity from several actual, real rotational recordings.

KEYWORDS: Diffraction, Free-Field, Half-Space, Elastic, Poroelastic

1. INTRODUCTION

After 75 years of strong-motion recording programs in the western United States, and during the last 40 years, in many other parts of the world, there are now well over several thousand strong motion accelerograms recorded, processed and available for distribution (Trifunac 2007). The observational strong motion programs evolved from realization in early 1900s that it is essential to record strong ground motions and structural response during actual earthquakes (Hudson, 1983a, b; Trifunac 2008a), to guide the development of the methods for analysis and prediction of structural response and to provide a basis for their experimental verification. The strong motion database accumulated so far allows earthquake engineers to 1) study the strong ground motion in different parts of the world, to understand its characteristics and destructive potential in relation to the tectonic characteristics of the areas where earthquakes occur; 2) to analyze and interpret the dynamic response of structures during earthquakes; 3) to identify and quantify the earthquake strong-motion parameters, associated with generation and transmission of strong motion waves, and 4) to provide a data bank

for future studies.

While the recorded data is invaluable for research and analyzes of strong-motion, it still does not cover many different recording conditions, which are needed for engineering design. This is particularly true in those regions, which have low seismic activity, and have not yet accumulated adequate strong motion database. It is also often necessary, to estimate future shaking at sites, which have characteristics outside the range of parameters for which the recorded data is now available. It is for these reasons that the development of modern empirical scaling equations for direct scaling of Fourier and response spectral amplitudes stated to appear following the successful multi-station recording of San Fernando, California, earthquake of 1971 (Trifunac 1976; Lee 2002a,b, 2007). This work on direct empirical scaling of spectral amplitudes also facilitated the development of the algorithms for generation of synthetic strong-motion accelerograms of translational components of strong motion (Trifunac 1971; Wong and Trifunac, 1979). It was also recognized that the torsional and rocking components of strong motion, acting together with the translations, can contribute significantly to the overall response of structures during strong earthquakes (Kobori and Shinozaki 1973; Luco 1976; Lee 1979). In absence of modern programs to develop strong-motion instruments to record the rotational components of strong-motion, it became necessary to estimate the rotational motions in terms of the corresponding translational motions. Trifunac (1982) showed how the torsion and rocking of ground surface associated with incident P, SV and SH waves can be determined in terms of the corresponding translational amplitudes of motions. Few years later Lee and Trifunac (1985, 1987), showed how to generate synthetic torsional and rocking accelrograms and their Fourier and response spectra, starting from the amplitudes of horizontal motions.

During the past two decades in spite of the fact that the engineering studies have continued to show the significance of the rotational components in strong motion excitation for the response of structures (Trifunac 2006, 2008b), the progress in developing and deploying strong motion instruments, which can also record rotational components of earthquake waves has continued to be slow.

In this paper we adopted our approach for the generation of artificial translational and rotational accelerograms, and present a physical, numerical method for its extension to generation of rotational Fourier spectra from that of recorded translational strong earthquake accelrograms, followed by examples of the estimated Foruier torsional and rocking spectra, and of their corresponding rotational time histories.

We have the following set of objectives in this paper:

- 1) To stress the importance of the rotational components of accelerograms, and promote the growth and development of strong-motion instruments for recording, together with the translational components, the rotational components of the accelerations of earthquake motions.
- 2) With the availability of rotational components of acceleration being so limited, we need to develop theories and algorithms for generating rotational motions from the corresponding available translational components of motions at each recording sites.
- 3) To use existing instrumentation to record, collect and process rotational time histories of acceleration in future seismic events if possible. This can then be used as a set of database to analyze and understand the rotational components of accelerograms, and to check the validity of developed theories of generating the rotational components of motions from translations.

An ongoing project, by one of the present authors of this paper, in Tianjin University of China, is the setting up of two six-component (three translational and three rotational components) sensors to record rotational components of free field and structures, respectively. The six-component sensor is a combination of EA-120 Force Balanced Accelerometer and R-1 Rotational Sensor. This will allow the recording of both the rotational and translational components. It is expected that the instrumentation may be of some help for the study of rotational ground motion.

2. FROM TRANSLATIONAL TO ROTATIONAL ACCELERATION SPECTRA

A comprehensive review of the general method for the generation of synthetic accelerogram, developed by the Strong Motion Research Group at the University of Southern California, can be found in Lee (2002). It generates synthetic translational accelerograms and uses the existing theory of linear, elastic wave propagation to generate the other accompanying components of strong motion, namely the rotational components of torsion and rocking, and the strains and curvatures.

2.1 Generation of Synthetic Torsional and Rocking Accelerograms

The importance of torsional and rocking excitations has been indicated by the studies of Dravinski and Trifunac (1979, 1980), Kobori and Shinozaki (1975), Luco (1976), Bielak (1978), Lee (1979), Gupta and Trifunac (1987, 1988, 1990a, 1990b, 1990c, 1991), Todorovska and Lee (1989), and Todorovska and Trifunac (1989, 1990a, 1990b, 1992, 1993). With the slow development of strong-motion instruments that record rotational components of strong motions (Hudson, 1983; Trifunac and Todorovska, 2001), it becomes necessary to explore the possibility of estimating those in terms of the corresponding translational components of strong shaking. By considering the horizontal propagation of plane waves with constant velocity C , Newmark (1969) estimated the contribution to the displacements of building foundation, resulting from torsional earthquake ground motions. Tso and Hsu (1978) used a similar approach, in addition to assuming that the motions also included plane non-dispersive waves. Nathan and MacKenzie (1975) discussed the possible averaging effects of foundation sizes on the resulting torsional excitations of buildings. These investigations, however, failed to consider the dependence of the phase velocity on the frequencies of the incoming Love waves. Their assumption that the incoming waves are of constant phase velocity at all frequencies, makes their results useless. Lee and Trifunac (1985) included the effects of wave dispersion and transient arrivals in the estimation of torsional accelerograms in an elastic layered half-space. The earlier work of Trifunac (1982) in calculating the torsional component of incident plane SH-waves was extended to enable the calculation of torsion from surface Love waves.

Lee and Trifunac (1985) extended the work of Wong and Trifunac (1978, 1979) in generating synthetic components of translational motions to that of Torsional motions. It was shown that the torsional motion $\psi(x, y, t)$ at the ground surface ($y = 0$) is related to the corresponding horizontal transverse displacement $w(x, y, t)$ by

$$\psi|_{y=0} = \frac{-i\omega}{2c_x} w|_{y=0} \quad (1)$$

where ω and c_x are respectively the frequency and phase velocity in the horizontal x - direction of the waves. This is applied in the frequency domain to the Fourier Transform of the synthetic components of acceleration.

Lee and Trifunac (1987) later further extended their work of the generation of synthetic Torsional motions above to that of generating synthetic rocking motions.. It was shown in a similar way that the rocking motion $\phi(x, y, t)$ at the ground surface ($y = 0$) is related to the corresponding vertical displacement $v(x, y, t)$ by

$$\phi|_{y=0} = \frac{i\omega}{c_x} v|_{y=0} \quad (2)$$

2.2 The Ratios of Rotational to Translational Fourier Spectra

The work of Lee and Trifunac (1985, 1987) allows the synthetic, artificial Rotational Fourier Spectra to be constructed together with the Translational Fourier Spectra using Eqn (1) for Torsional Spectra and Eqn (2)

for Rocking Spectra. From the Rotational Fourier Spectra, Inverse Fourier Transform will generate the corresponding synthetic Torsional and Rocking acceleration time histories. This procedure can then be adopted and modified to generate estimated Rotational Fourier Spectra from actual translational Fourier Spectra computed from actual recordings

Equation (1), for example, shows that the ratio of the Fourier spectra of Torsional motion, $\Psi(\omega)$, to that of the corresponding transverse horizontal motion, $H(\omega)$ is

$$\frac{\text{Torsion FS}}{\text{Horizontal FS}} = \frac{\Psi(\omega)}{H(\omega)} = \frac{-i\omega}{2c(\omega)}, \quad \text{with amplitude} \quad \left| \frac{\Psi(\omega)}{H(\omega)} \right| = \frac{\omega}{2c(\omega)} \quad (3)$$

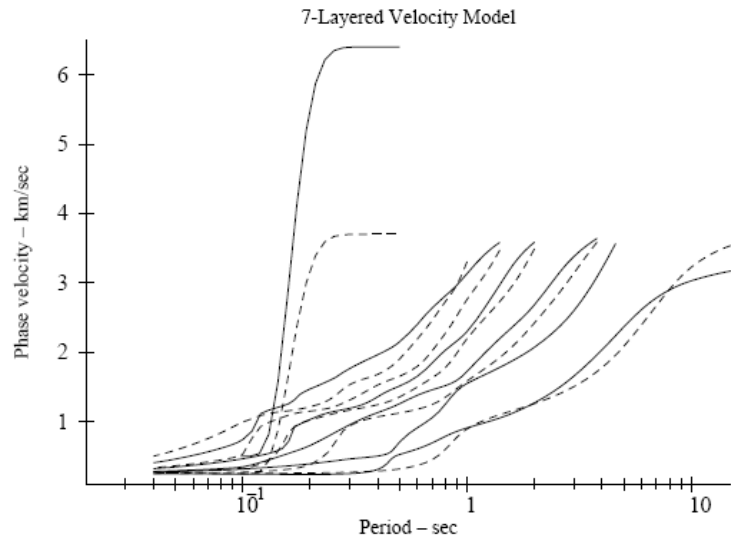
where $c(\omega)$ is the horizontal phase velocity.

Table 1 Layered Medium near El Centro, California.

Layer #	Depth (km)	c_α	c_β	Density (gm/cc)
1	0.05	0.60	0.30	1.20
2	0.13	1.70	0.98	1.28
3	0.55	1.96	1.13	1.36
4	0.98	2.71	1.57	1.59
5	1.19	3.76	2.17	1.91
6	2.68	4.69	2.71	2.19
7	∞	6.40	3.70	2.71

c_α, c_β : P, S-Wave Velocities, (km/sec)

Figure 1



As an illustration we consider a 7 Layer model (Table 1). It corresponds to a site in El Centro, California. Dispersion curves for this site were computed using the Haskell-Thomson matrix method (Haskell, 1953; Thomson, 1950), which generated the phase and group velocity curves for Rayleigh and Love waves. The 5 solid curves in Fig. 1 from the right are for the first five modes of the Rayleigh waves. Mode 1 is the rightmost solid curve, followed by Modes 2 to 5 to the left. The same holds for the five modes of Love waves, which are plotted with dashed lines. At short periods, all curves approach the minimum shear S -wave velocity (in this example 0.30 km/s). The two leftmost curves are the corresponding body waves, with the dashed S -wave below the solid P -wave on top. The body S -wave starts at the minimum c_β , 0.3 km/s at period near 0.1sec and quickly rises to the maximum c_β , 3.7 km/s. The body P -wave similarly starts at the minimum c_α , 0.6 km/s and quickly rises up to the maximum c_α , 6.4km/s. They will be included with the surface waves respectively as the 6th and 7th modes of waves.

Next we consider the transverse components of Love waves and the corresponding torsional waves. Lee and Trifunac (2008) noted, the waves corresponding to their m^{th} mode, defined (only) within the frequency band, $\omega_n \pm \Delta\omega_n$, are

$$\frac{\Psi_{nm}(\omega)}{H_{nm}(\omega)} = \frac{-i\omega}{2c_{nm}}, \quad \text{with amplitude} \quad \left| \frac{\Psi_{nm}(\omega)}{H_{nm}(\omega)} \right| = \frac{\omega}{2c_{nm}} \quad (4)$$

where $c_{mm} = c_m(\omega_n)$ is the Love wave phase velocity of m^{th} mode at frequency $\omega = \omega_n$, $H_{mm}(\omega)$ and $\Psi_{mm}(\omega)$ are respectively the m^{th} mode of the Translational and Rotational Fourier Spectra from the surface Love waves.

Figure 2 shows a plot of these ratios, $\omega/2c_m(\omega)$, for the five modes of Love waves plus body S-waves as the 6th mode. The curves for the 6 modes all have similar slopes, especially at high frequency, along the “diagonal” green line, a straight line joining the limits of $\omega/2\beta_{\max}$ at the low frequency end and $\omega/2\beta_{\min}$ at the high frequency end. This is an important “linear trend”, which will be used.

A simple way to characterize the ratio, $\Psi(\omega)/H(\omega)$, with all the modes of Love waves combined, within $\omega_n \pm \Delta\omega_n$, would be to write (Lee and Trifunac, 2008):

$$\left. \frac{\Psi(\omega)}{H(\omega)} \right|_{\omega=\omega_n} = \frac{\Psi(\omega_n)}{H(\omega_n)} = \left. \frac{\Psi_n(\omega)}{H_n(\omega)} \right|_{\omega=\omega_n} = \frac{-i\omega_n}{2\bar{c}_n} \quad (5)$$

where $\bar{c}_n = \bar{c}(\omega_n)$, and $1/\bar{c}_n$ represent weighted average of the phase velocities of all the modes of Love waves at frequency ω_n . Note that this ratio is dependent only on the frequency and the local phase velocity spectra of the surface Love waves at the site.

\bar{c}_n can be viewed as the weighted average of the phase velocities $c_{mm} = c_m(\omega_n)$ at frequency $\omega = \omega_n$ of the 5 modes of surface Love waves plus body S-wave. The dashed line as ratio of amplitudes $\omega/2\bar{c}(\omega)$ will thus be running very close along the dashed line from $\omega/2\beta_{\max}$ at low frequencies to $\omega/2\beta_{\min}$ at high frequencies.

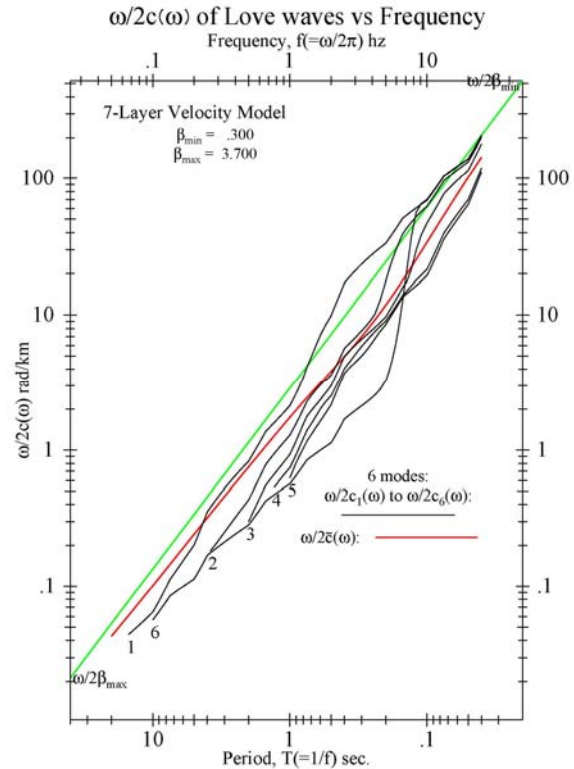
In exactly the same way, the spectra of rocking, $\Phi(\omega)$, can next be expressed in terms of the spectra of the vertical translation, $V(\omega)$. The vertical translational Fourier spectrum is now composed of modes of Rayleigh surface waves. Now

$$\left. \frac{\text{Rocking FS}}{\text{Vertical FS}} \right|_{\omega=\omega_n} = \left. \frac{\Phi(\omega)}{V(\omega)} \right|_{\omega=\omega_n} = \frac{\Phi(\omega_n)}{V(\omega_n)} = \left. \frac{\Phi_n(\omega)}{V_n(\omega)} \right|_{\omega=\omega_n} = \frac{i\omega_n}{\bar{c}_n}, \quad (6)$$

with $\bar{c}_n = \bar{c}(\omega_n)$, representing the weighted average of the M modes of Rayleigh waves.

Recall that these ratios of Rotational to Translational Fourier Spectra (Equation (5) for Torsion, and Equation (6) for Rocking) are dependent only on the phase velocity spectra, $\bar{c}_n = \bar{c}(\omega_n)$, at the site and are independent of the input translational acceleration. In other words, for the same site, the ratios of Rotational to Translational Fourier Spectra are always given by Equations (5) and (6), dependent only on the local geology at

Figure 2



the site.

Such ratios can be estimated at each site by generating the synthetic Rotational and Translational acceleration (Lee and Trifunac, 1985, 1987) Spectra and taking their ratios.

With these ratios available at a given site, and if an actual accelerogram recording is available at the same site, they can next be applied to calculate the rotational Torsional and Rocking Fourier Spectra from the actual Translational Fourier Spectra. The corresponding rotational time histories can then be calculated using Inverse Fourier Transform.

3. EXAMPLE: ROTATIONAL SPECTRA AT PACOIMA DAM, CALIFORNIA

Figure 3

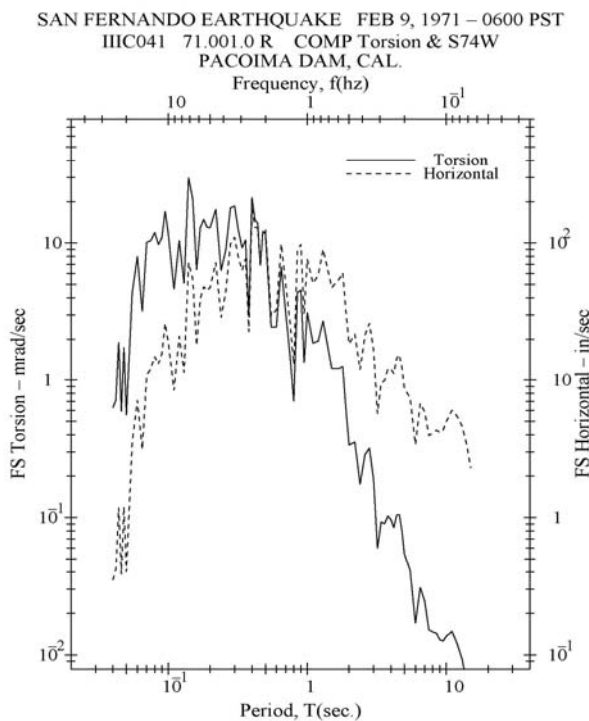
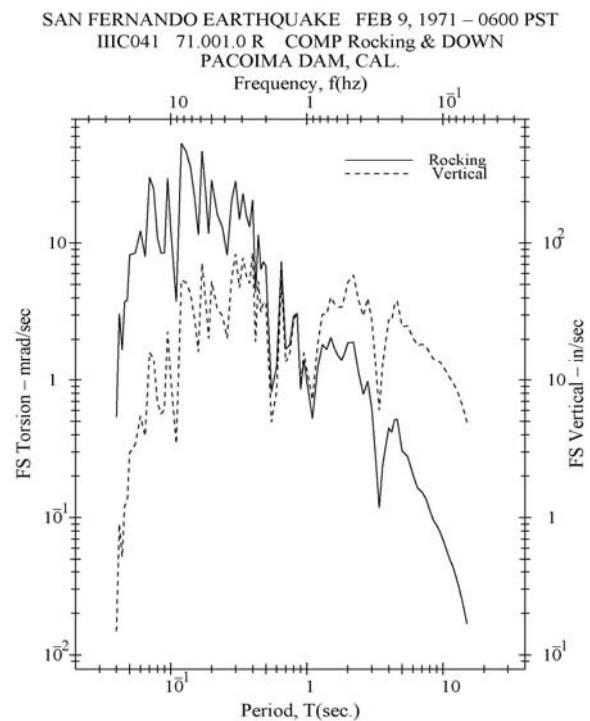


Figure 4



Here's an example of the estimation of rotational spectra from the translational components of the Fourier spectra of record strong motion. We illustrate this for accelerogram recorded at Pacoima Dam, in California, during the Feb 9, 1971 San Fernando Earthquake. Its S74W (horizontal) component had a peak acceleration of $1055. \text{ cm/sec}^2$, while the vertical component had a peak acceleration of 696.0 cm/sec^2 . The Fourier spectra of these two horizontal (as the transverse) and vertical components can be used to estimate the corresponding torsional and rocking components of motion. Figure 3 shows a plot of the Fourier Spectrum amplitudes of the horizontal component S74W in units of in/sec and the corresponding torsional component in units of mrad/sec (10^{-3} rad/sec). Figure 4 shows the plot of the Fourier Spectrum amplitudes of the vertical component of acceleration, and of the corresponding rocking component. The geological velocity profile of Table I is used, where the minimum and maximum shear wave velocities, β_{\min} and β_{\max} , range from 0.30 km/sec to 3.70 km/sec.

Figures 5 and 6 show the corresponding rotational torsional and rocking time histories obtained from the inverse FFT of the corresponding rotational spectra in Figures 3 and 4. The rotational acceleration, velocity and

displacement are respectively given in units of mrad/s/s, mrad/s and mrad, where 1 mrad = 0.001 rad. The peak rotations of 0.3 mrad for torsion and 0.6 mrad for rocking are obtained from the calculations.

Figure 5

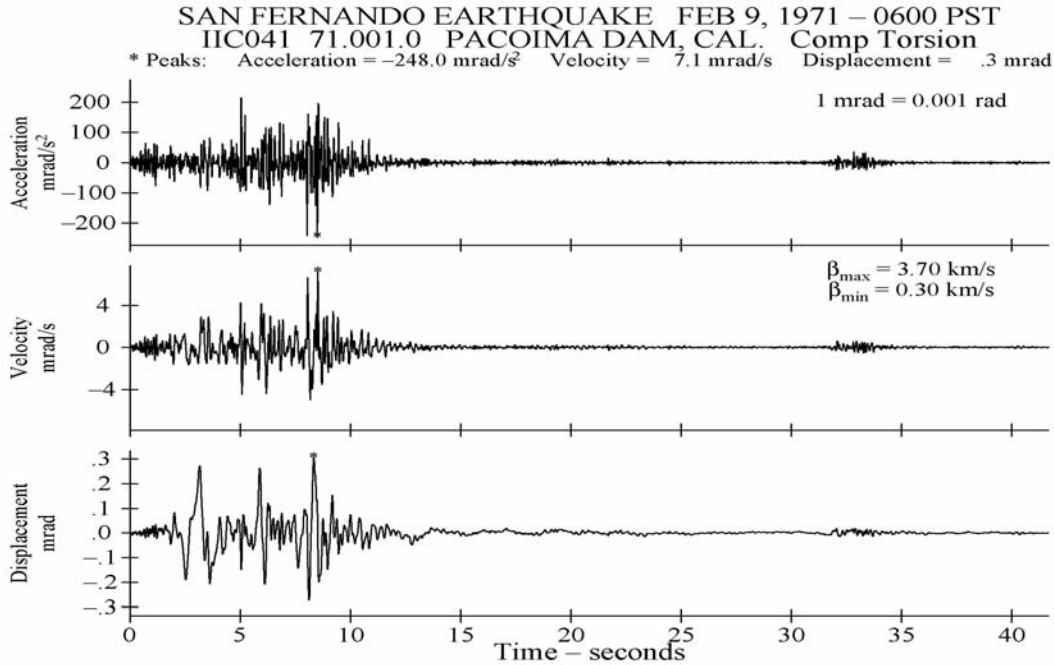
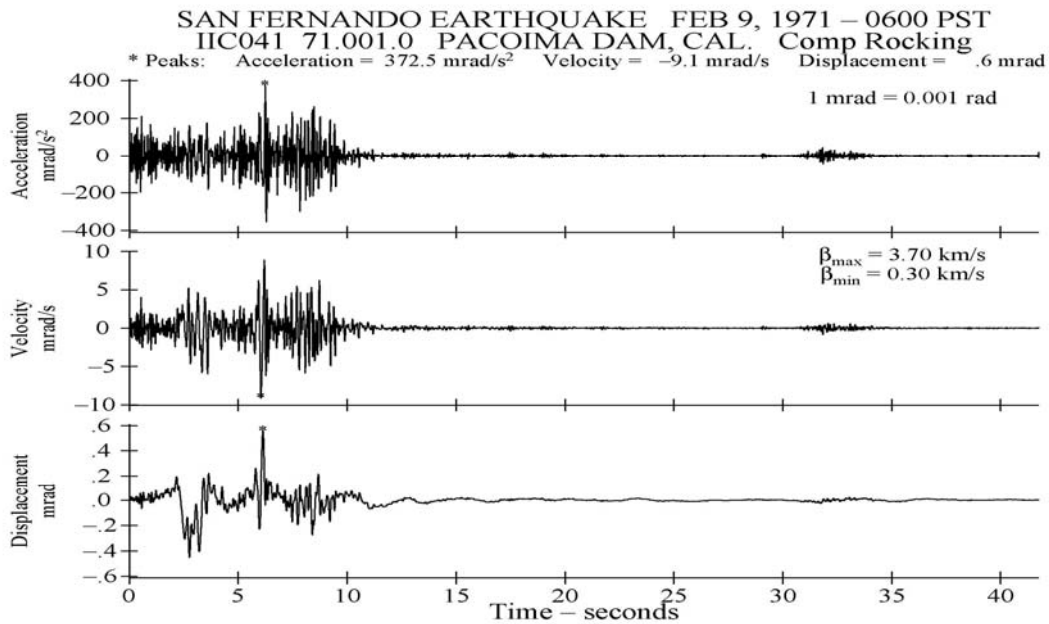


Figure 6



It is seen that one can use this procedure to generate estimated time histories for torsional and rocking motions for every recorded translational accelerogram for which the site geological data are available. Further work and approach can be found in Lee and Trifunac, 2008. Next we'll wait for the actual recording of translational and rotational data to be compared with the estimated data by this procedure.

REFERENCES

- Bouchon, M., and Aki, K. (1982).** Strain and rotation associated with strong ground motion in the vicinity of earthquake faults. *Bull. Seism. Soc. Am.* **72(5)**, 1717–1738.
- Graizer, V.M. (2006).** Tilts in strong ground motion. *Bull. Seism. Soc. Am.*, **96(6)**, 2090–2102.
- Haskell, N.A. (1953).** The Dispersion of Surface Waves on Multilayered media, *Bull. Seism. Soc. Am.*, **43**: 17-34.
- Hudson, D. E. (1983a)** History of Accelerograph Development, *Proc. of the Golden Anniversary Workshop on Strong Motion Seismology*, U.S.C., 29-56.
- Hudson, D. E. (1983b).** Strong Motion Instrumentation Systems, *Proc. of the Golden Anniversary Workshop on Strong Motion Seismology*, U.S.C., 73-86.
- Kobori, T. and Shinozaki, I. Torsional (1973).** Vibration of Structure Due to Obliquely Incident SH Waves, *Proc. Fifth World Conf Earthquake Eng.* 1(22).
- Lee, V. W. (1979).** Investigation of Three-Dimensional Soil-Structure Interaction, Dept. of Civil Eng. *CE 79-11*, University of Southern California, Los Angeles, 1979
- Lee, V.W. (2002a).** Empirical Scaling of Strong Earthquake Ground Motion: Part I: Attenuation and Scaling of Response Spectra, *ISET J. Earthquake Technology*, **39(4)**. 219–254.
- Lee, V.W. (2002b)** Empirical Scaling of Strong Earthquake Ground Motion: Part III: Synthetic Strong Motion, *ISET J. Earthquake Technology*, **39(4)**, 273-310.
- Lee, V.W. (2007).** Empirical Scaling of Strong-Motion Response Spectral Amplitudes - a Review *ISET J. Earthquake Technology*, 44(1) Special Issue 39-69.
- V. W. Lee and M.D. Trifunac (1985).** [Torsional Accelerograms](#), *Int. J. Soil Dynamics & Earthquake Eng.*, 4(3), 132-139.
- Lee, V. W. and M.D. Trifunac (1987)** Rocking Strong Earthquake Accelerations, *Int. J. Soil Dynamics & Earthquake Eng.*, **6(2)**, 75-89.
- Lee, V.W. and Trifunac, M.D. (1995).** Frequency Dependent Attenuation Function and Fourier Amplitude Spectra of Strong Earthquake Ground Motion in California, *Report CE 95-03*, Dept. of Civil Eng., Univ. of Southern California, Los Angeles, CA.
- Lee, V.W. and Trifunac, M.D. (2008).** Empirical Scaling of Rotational Spectra of Strong Earthquake Ground Motion, BSSA Special Issue on "Rotational Seismology and Engineering Applications (in review).
- Luco, J. E. (1976).** Torsional Response of Structures for SH Waves The Case of Hemispherical Foundation, *Bull. Seism. Soc. Amer.* **66**, 109-123.
- Takeo, M. (2006).** Ground rotational motions recorded in near-source region of earthquakes, Ch. 12 in the book *Earthquake Source Asymmetry, Structural Media and Rotation Effects*, R. Teisseyre, M. Takeo, and E. Majewski (eds.). Springer, Heidelberg, Germany, 157–167.
- Takeo, M., and Ito, H.I. (1997).** What can be learned from rotational motions excited by earthquakes?, *Geophys. Jour. Int.*, **129**, 319–329.
- Thomson, W.T. (1950).** Transmission of Elastic Waves through a Stratified Solid Medium, *J. Appl. Phys.*, **21**: 89-93.
- Trifunac, M.D. (1971)** A Method for Synthesizing Realistic Strong Ground Motion, *Bull. Seism. Soc. Amer.*, **61**, 1739-1753.
- Trifunac, M.D. (1972).** Stress Estimates for San Fernando, California Earthquake of February 9, 1971: Main Event and Thirteen Aftershocks, *Bull. Seism. Soc. Amer.*, **62(3)**, 721-750.
- Trifunac, M.D. (1974).** A Three-Dimensional Dislocation Model for the San Fernando, California, Earthquake of February 9, 1971, *Bull. Seism. Soc. Amer.*, 64(1), 149-172.
- Trifunac, M.D. (1976).** Preliminary Empirical Model for Scaling Fourier Amplitude Spectra of Strong Ground Acceleration in Terms of Earthquake Magnitude, Source to Station Distance and Recording Site Conditions, *Bull. Seism. Soc. Amer.*, **66(4)**, 1343-1373.
- Trifunac, M. D. (1982)** A Note on Rotational Components of Earthquake Motions on Ground Surface for Incident Body Waves, *Soil Dynamics and Earthquake Engineering* 1(1), 11-19.



- Trifunac, M.D. (1989a).** Dependence of Fourier Spectrum Amplitudes of Recorded Strong Earthquake Accelerations on Magnitude, Local Soil Conditions and On Depth of Sediments, *Int. J. Earthquake Eng. and Structural Dyn.*, **18**(7), 999-1016.
- Trifunac, M.D. (1989b).** Empirical Scaling of Fourier Spectrum Amplitudes of Recorded Strong Earthquake Accelerations in Terms of Magnitude and Local Soil and Geologic Conditions, *Earthquake Eng. and Eng. Vibration*, **9**(2), 23-44.
- Trifunac, M.D. (1990).** How to Model Amplification of Strong Earthquake Motions by Local Soil and Geologic Site Conditions, *Int. J. Earthquake Eng. and Structural Dynamics*, **19**(6), 833-846.
- Trifunac, M.D. (1991).** Empirical Scaling of Fourier Spectrum Amplitudes of Recorded Strong Earthquake Accelerations in Terms of Modified Mercalli Intensity, Local Soil Conditions and Depth of Sediments, *Int. J. Soil Dynamics and Earthquake Eng.*, **10**(1), 65-72.
- Trifunac, M.D. (2006).** Effects of Torsional and Rocking Excitations on the Response of Structures, Ch. 39 in the book *Earthquake Source Asymmetry, Structural Media and Rotation Effects*, Edited by R. Teisseyre, M. Takeo, and E. Majewski, Springer, Heidelberg, Germany, 569-582.
- Trifunac, M.D. (2007).** Recording Strong Earthquake Motion – Instruments, Recording Strategies and Data Processing, Dept. of Civil Engineering, Report CE 07-03, Univ. Southern California, Los Angeles, California.
- Trifunac, M.D. (2008a).** 75th Anniversary of Strong Motion Observation – A Historical Review, (submitted for publication).
- Trifunac, M.D. (2008b).** Buildings as Sources of Rotational Waves, Chapter I.5 in *Physics of Asymmetric Continua: Extreme and Fracture Processes*, edited by R. Teisseyre, H. Nagahama, and E. Majewski, Springer, Heidelberg, Germany, (in press).
- Trifunac, M.D. (2008c).** The Role of Strong Motion Rotations in the Response of Structures near Earthquake Faults, *Soil Dynamics and Earthquake Engineering*, (in press).
- Trifunac, M.D., and Hudson, D.E. (1971).** Analysis of the Pacoima Dam accelerogram, San Fernando, California earthquake of 1971. *Bull. Seism. Soc. Amer.*, **61**(5), 1393–1411.
- Wong, H.L., and M.D. Trifunac (1979).** Generation of Artificial Strong Motion Accelerograms, *International Journal of Earthquake Engineering and Structural Dynamics*, **7**, 509-527.